

UDC 621.3

T. Thieme

LBA DIFFERENTIAL PRESSURE SENSORS HIGH IMMUNITY TO DUST CONTAMINATION

In this paper First Sensors LBA differential pressure (ΔP) sensors are experimentally compared to other sensors which use the same (thermal-anemometer-based, non-membrane) sensing principle, where differential pressure is inferred from a gas flow through the sensor.

LBA; DIFFERENTIAL PRESSURE SENSORS; FIRST SENSORS; GAS FLOW THROUGH.

T. Tume

ВЫСОКАЯ УСТОЙЧИВОСТЬ ДИФФЕРЕНЦИАЛЬНЫХ СЕНСОРОВ ДАВЛЕНИЯ СЕРИИ LBA К ПЫЛЕВОМУ ЗАГРЯЗНЕНИЮ

В статье представлены результаты экспериментального сравнения дифференциальных сенсоров давления серии LBA компании First Sensors с иными сенсорами, в которых использован тот же принцип действия (термо-анемометрические, безмембранные): перепад давления определяется методом продувки газа через сенсор.

LBA; ДИФФЕРЕНЦИАЛЬНЫЕ СЕНСОРЫ ДАВЛЕНИЯ; FIRST SENSORS; МЕТОД ПРОДУВКИ ГАЗА.

With dust in the air flow, all other sensors having flow impedance 15 Pa/(ml/s) to 300 Pa/(ml/s) went out of calibration or failed entirely while the LBA sensors having flow impedance >10 kPa/(ml/s) kept their calibrated sensitivity. First Sensors LBA ΔP sensors require only very tiny flows through its body and therefore provide high immunity to dust-bearing air.

Introduction. The LBA series low-pressure sensors with ranges from 25 Pa (0.1 inH₂O) full scale sense differential air or gas pressure, inferring differential pressure from nano-liters per second gas flow through an integrated air-flow channel having high flow impedance. The transducer is a MEMS-based thermo-anemometer on a monolithic silicon chip. Rejutor technology combined with CMOS circuitry provides on-chip-integrated analog-only compensation and conditioning electronics.

Flow-Through Leakage. Because of the sensing mechanism, there is nonzero air-flow leakage through the sensor itself during operation. This is true of all differential pressure sensors using the thermal-anemometer sensing

principle, (as opposed to dead-end sensors such as piezo-resistive membrane-based sensors, whose sensing element does not leak). Still, thermal-anemometer-based ΔP sensors have considerable success in the marketplace, because they enable practical and cost-effective sensing of very low ΔP , such as a few hundred Pa full-scale and below.

In this context, the question arises, how much flow-through leakage is too much? The answer depends on details of the application, and on how the ΔP sensor is connected and used.

Being able to measure differential gas pressures below a few hundred Pa, with resolution better than 0.1 Pa, these sensors may be affected by other components of the measurement system such as connecting pipes/tubes and filters, and by the quality of the gas which may contain dust, humidity or liquid droplets.

Some manufacturers of thermal-anemometer-based ΔP sensors recommend the use of connection tubes having a particular length, in order to avoid distortion of the response of the manufacturer-calibrated sensors.

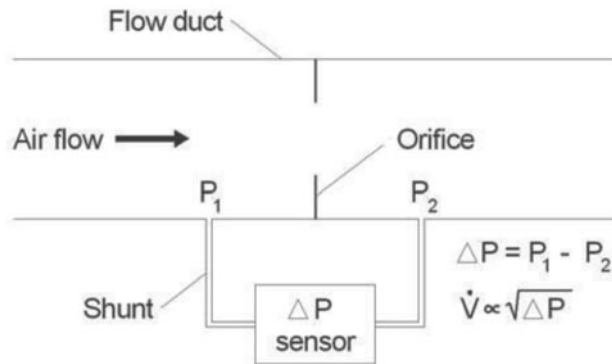


Fig. 1. Typical volumetric flow measurement set-up with differential pressure sensor

Manufacturers also may recommend the use of dust filters, or may use dust-segregation elements/mechanisms as part of their sensors. Note that these types of precautions are not needed for membrane-type sensors where the gas flow through the connection tubing is zero (in static mode).

In general, designers of a flow-measurement system using a thermal-anemometer-based differential pressure sensor must consider factors caused by nonzero gas flow through the sensor, in order to provide reliable long-term operation. Unfortunately, there are no standard test/certification procedures and detailed technical information to address these issues. The tests described below were performed with thermal-anemometer-based sensors from different manufacturers, to demonstrate the principal importance of the

flow-through leakage (pneumatic impedance, or flow impedance) of the sensors, for reliable operation in practical applications.

Note: The pneumatic impedance R_{pn} of the sensor, measured in $[kPa/(ml/s)]$, determines the gas flow through the sensor at a certain pressure drop, ΔP s across the sensor:

$$\text{Flow-through leakage} = \frac{\Delta P}{R_{pn}}$$

Flow Measurement Using Differential Pressure Sensors. Micro-flow-based differential pressure sensors are typically used to measure differential pressure generated by gas flow passing through an air-flow duct or “flow tube”. Examples are respiratory flow measurement in medical ventilators as well as air flow measurement or filter control in HVAC applications.

Consider, for example, the sensor being used

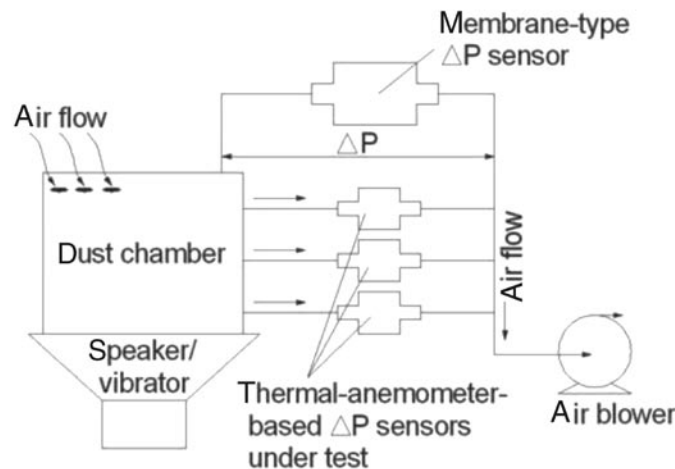


Fig. 2. Schematic diagram of horizontal configuration

in a shunt configuration, to sense differential pressure $\Delta P = P_1 - P_2$ across a flow-restrictive element in an air duct, thereby inferring measurement of air flow in the duct as shown in Fig. 1. Such conversion elements, designed for different applications, include orifices, baffles, Pitot tubes, Venturi tubes, calibrated diaphragms, and special flow-to-pressure converters used in respiration equipment such as Fleisch or Lilly tubes.

LBA differential pressure sensors feature very high flow-through impedance, greater than 10 kPa per (ml/s) for the most-sensitive models and up to hundreds of kPa/(ml/s) for higher full-scale ranges.

In principle, these sensors with high flow impedance need less parasitic flow in order to make a measurement, and thus cause less disturbance to the main flow than other sensors with lower flow impedance. This makes the sensor virtually equivalent to membrane-type (dead-end type) differential pressure sensors regarding this important aspect of performance for many applications.

Risk From Dust Contamination. In applications such as HVAC, where dust particles may be present in the main air flow, the question may naturally arise whether such dust presents a reliability hazard to thermal-anemometer-based sensors. Since normal function of the sensor involves air flow through the flow-channel, it is certainly plausible that such air flow may carry dust particles into the sensor's flow channel. Thus the hypothetical dangers from dust particles are that they could enter the sensor's flow-channel, causing:

- A change (increase) in the sensor's internal flow impedance and therefore a change (decrease) in the sensor's calibrated sensitivity. This would be seen as a reduction in the sensor's output voltage, for a given applied ΔP , and a loss of calibration;
- A complete blockage of the sensor's internal flow channel (functional failure);
- Dust may adhere on or near to the sensitive microstructures that make up the sensing element inside the channel, causing a change in calibration.

In general, the presence of dust may in principle present a reliability hazard, but the extent of the hazard is primarily determined

by the flow-through impedance (pneumatic impedance) of the sensor.

Risk Factors Dust quantity and air velocity.

The quantity of dust particles which the air flow brings to the input of the sensor depends on the volume of air passing through the sensor and depends on the velocity of air flow. The quantity of dust particles induced to travel into the sensor's air flow channel depends on the quantity of dust particles which are present at its input, and on the velocity of air flow into the channel. The velocity of air flow toward the sensor has another very important effect, beyond simple volume of air transported to and into the sensor. If the airflow velocity is slow enough that the dust does not remain airborne, this may further enhance the sensor's immunity to dust contamination, while if the air flow velocity toward the sensor is great enough that the dust remains in suspension, this may tend to degrade the sensor's immunity to dust contamination.

Note:

The sensor's flow-impedance directly affects the velocity of approaching airflow. Thus, high flow impedance in the sensor both reduces the volume of air passing through the sensor's channel, and reduces the velocity of the approaching air, potentially allowing airborne dust to settle out, as well as reducing the force on particles already present at the input of the sensor.

Type of dust. For example, big and heavy dust particles are less likely than small/light particles, to be transported through the tubing to the sensor. Also, the size of the dust particles affects whether the dust can physically block air flow into the sensor's flow channel, and whether the dust can physically enter the sensor's flow channel.

Concentration of dust particles in the main flow. The concentration of dust reaching the sensor depends on the concentration of dust in the main gas flow.

Connection of the sensor to main flow duct.

Referring to Fig. 1, the larger the inner diameter of the connection tubing, the lower will be the linear velocity of the gas flow of dust-bearing air toward the sensor input. Also, the longer the connection tubing, the greater will be the flow impedance contributed by that connection tubing, and this may in turn affect the

linear velocity of the gas flow of dust-bearing air toward the sensor input.

Also, the presence of dust collectors (such as gravity-traps) and dust filters, can provide a certain level of protection for the sensor against dust.

Note:

The goal of this experiment is to estimate and compare the immunity of the sensor itself to dust contamination. Improvements related to dust filtering and other additional protection of the sensors are outside the scope of the present investigations.

Experimental Investigation of Dust Contamination. In order to investigate the risk presented by dust, comparative experimental studies were conducted.

The experimental setup was designed and built to provide reproducible and controllable conditions for the tested sensors, and to allow fair comparative analysis of different sensors. With this target, sets of ΔP sensors using the thermal-anemometer sensing principle were subjected to common applied differential pressures.

In each experiment, typically two or more sensor samples, often having different flow impedances, were connected in parallel such that a common differential pressure was present across all sensors.

Type of Test Dust. At the pressure port receiving the higher applied pressure, a source of airborne dust was connected.

The dust was purchased from a supplier of test dust. The test dust product was, specifically “ISO 12103-1, A2 Fine Test Dust” having particle size distributed between less than $1\ \mu\text{m}$ (less than 3.5 % volume) and approximately $100\ \mu\text{m}$, with roughly uniform volume-distribution between $\sim 5\ \mu\text{m}$ and $\sim 40\ \mu\text{m}$.

The chemical composition of the test dust was

SiO ₂	68-76 %
Al ₂ O ₃	10-15 %
Fe ₂ O ₃	2-5 %
Na ₂ O ₃	2-4 %
CaO	2-5 %
MgO	1-2 %
K ₂ O	2-5 %
TiO ₂	0,5-1 %

Experimental setup. In the first configuration (Fig. 2), the sensors under test were arranged horizontally, at the same level as the dust chamber and all at the same level to each other.

In the second configuration (Fig. 3), the sensors under test were arranged vertically, such that the dust-bearing air had to flow upward from the dust chamber toward the sensors. In this configuration, it is expected that the effect of

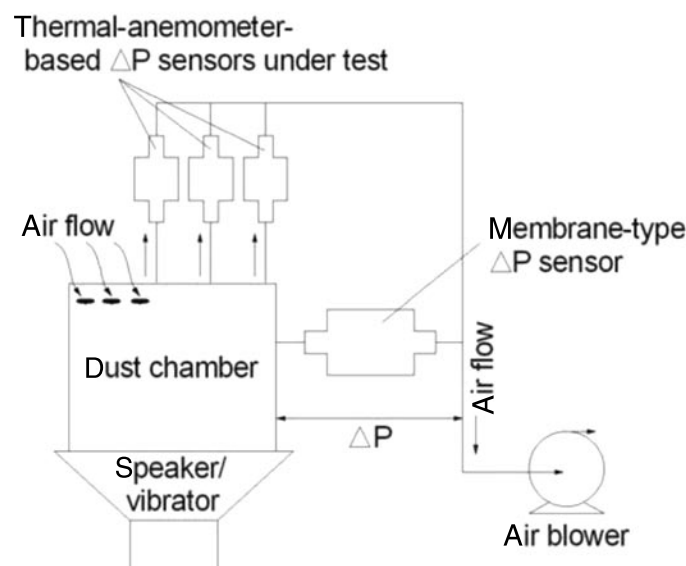


Fig. 3. Schematic diagram of vertical configuration

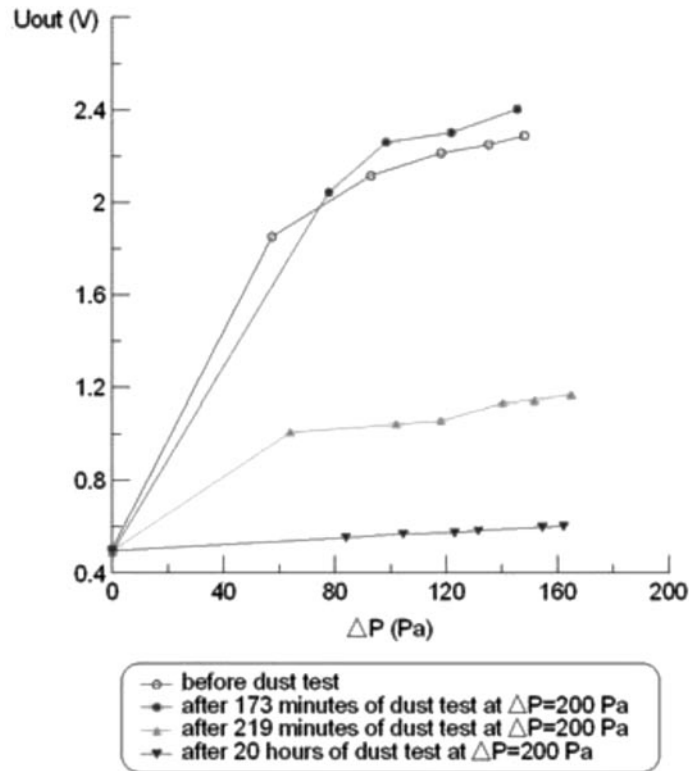


Fig. 4. Test #1 results for Sensor 2-1 (horizontal orientation of the sensor)

gravity will be to delay and reduce particle flow toward the sensors under test, thus offering to the sensors some amount of “protection” from dust contamination. It was attempted to avoid turbulent flow patterns which could artificially distort the spatial distribution of dust.

Test conditions. In each configuration, several sensors under test were connected in parallel with a commercially calibrated membrane-type ΔP sensor (unaffected by dust). Note that the common ΔP is necessarily applied to each sensor under test plus a small length (~5 inches) of connection tubing for each sensor. The connection tubing was 1/8” ID. With the goal of generating a reproducible concentration of dust in the air, a quantity of dust (~10 cm³) was placed in a chamber having a volume of a few hundred cm³.

The chamber was agitated continually at 20 Hz using triangular-shaped mechanical pulses with an amplitude of ~1 mm, using a common low-frequency audio speaker (subwoofer). The chamber has ventilation holes, to allow air flow at atmospheric pressure into and through the chamber

toward one port of the sensors under test.

A regulated air blower generated a constant vacuum pressure applied to the other port of each sensor under test. This vacuum pressure “pulled” air from the dust chamber through all the connected sensors simultaneously. The magnitude of this air flow, through each individual sensor, is inversely proportional to the flow impedance of each individual sensor.

Sensors under test. Several commercially-available sensors from several different manufacturers were comparatively examined:

- First Sensors LBA sensors with measurement range 0...250 Pa (1 inH₂O full-scale), flow impedance ~80 kPa/(ml/s), and integrated analog conditioner with 0.5...4.5 V output.

Sample ID: LBAS250UF6S (# 1)

Sample ID: LBAS250UF6S (# 2)

- First Sensors LBA sensors with measurement range 0...50 Pa (0.2 inH₂O full-scale), flow impedance ~30 kPa/(ml/s), and integrated analog conditioner with 0.5...4.5 V output.

Sample ID: LBAS050UF6S (# 1)

- Manufacturer #1 sensors with measurement range 0...±20 Pa (±0.8 inH₂O full-scale), flow impedance ~15 Pa/(ml/s), and unamplified analog output ±70 mV.

Sample ID: Sensor 1-1

Sample ID: Sensor 1-2

- Manufacturer #2 sensors with measurement range 0...200 Pa (0.8 inH₂O full-scale), flow impedance ~15 Pa/(ml/s), and amplified analog output 0.5...4.5 V. These sensors have a micro-apparatus for dust separation, internal to the sensors flow channel.

Sample ID: Sensor 2-1

Sample ID: Sensor 2-2

Sample ID: Sensor 2-3

- Manufacturer #3 sensors with measurement range -20...+500 Pa (2 inH₂O full-scale), flow impedance ~300 Pa/(ml/s), and integrated conditioner with 0.25...4.25 V output.

Sample ID: Sensor 3-1

Sample ID: Sensor 3-2

Test procedure. The sensors were compared in subgroups of 2 to 4, subjected to a common ΔP. The common ΔP was typically near the full-scale of the sensor having the greatest full-scale of the sub-group. While the pump was pulling dust-bearing air through the sensors, several voltage signals were monitored continually and stored:

- The voltage output from the membrane-based ΔP sensor (as a control);
- The voltage output from each sensor under test.

Note:

In cases where the full-scale ranges of the sensors were not the same, and where the applied ΔP was set near to the full-scale of the sensor with greater full-scale, the sensor with lower full-scale has saturated output voltage and cannot be effectively monitored without interrupting the test to reduce the flow. Thus there were typically several interruptions, at intervals during each test.

For each sensor under test, the output voltage vs. applied differential pressure was coarsely

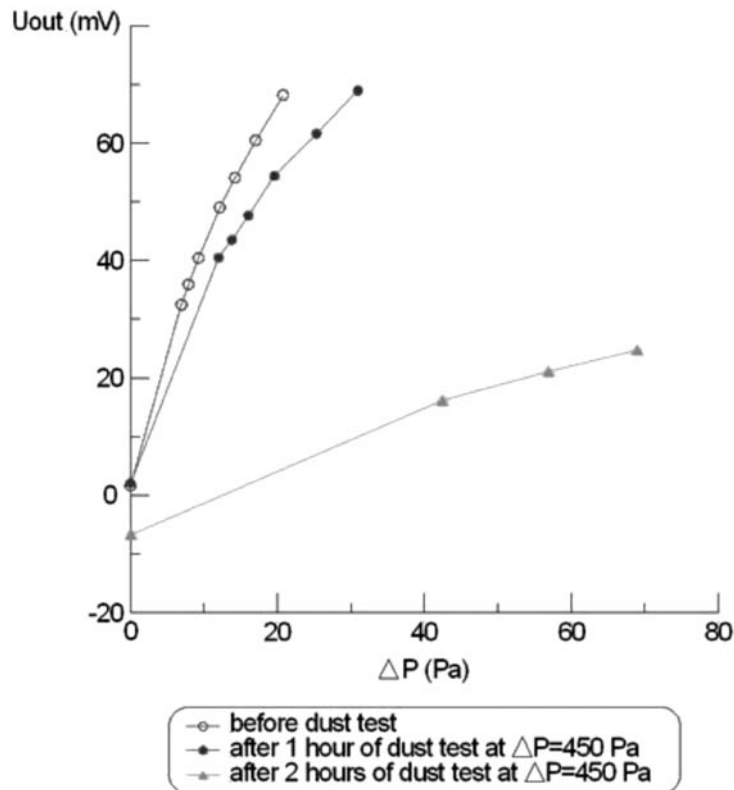


Fig. 5. Test #2 results for Sensor 1-1 (horizontal orientation of the sensor)

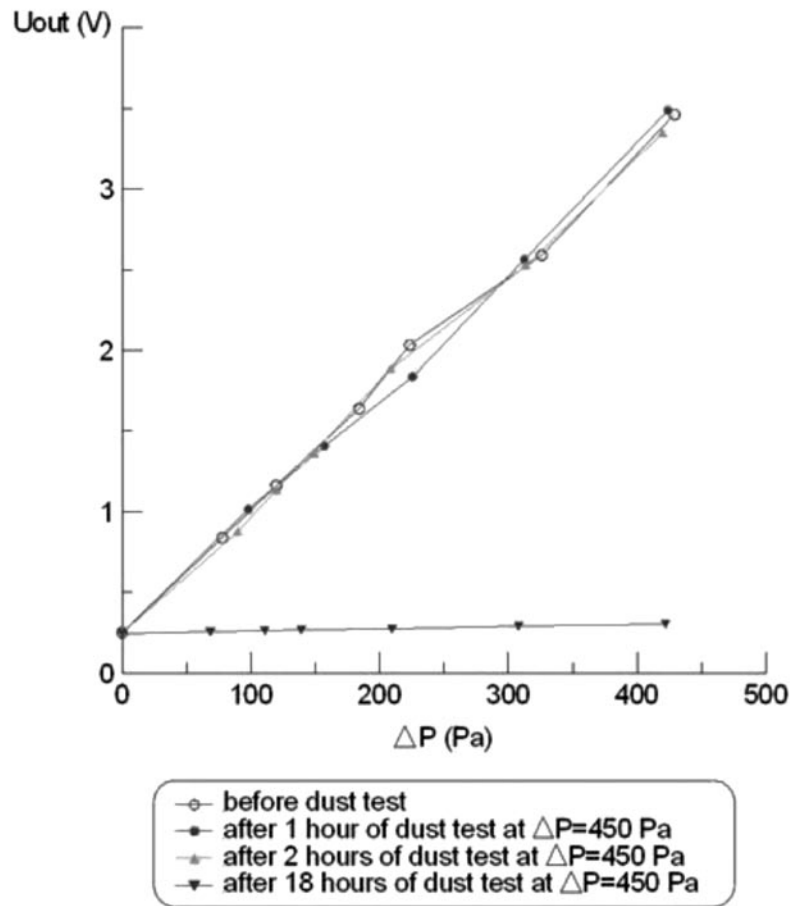


Fig. 6. Test #2 results for Sensor 3-1 (horizontal orientation of the sensor)

characterized using the above-described setup, by changing the pump settings to pull varying amounts of pressure across the sensors. This coarse-characterization was done before the dust test began, at various intervals throughout the dust-test, and then after the end of the dust test. Additionally, for each LBA sensor under test, the output voltage was measured as a function of accurately measured applied pressure, before the dust test began, and again after the end of the dust test, to confirm the coarse-characterization results, and to show the effect of the accumulated dust exposure on sensor samples whose output voltage was saturated during the actual dust exposure.

Test #1. In the first test, sensors LBAS250UF6S (# 2), LBAS050UF6S, and Sensor 2-1 were connected in parallel to the dust chamber, in the first configuration shown in Fig. 2 (with the sensors arranged horizontally

at the same level as the dust chamber).

The test was run for 20 hours at a constant differential pressure $\Delta P = 200$ Pa (0.8 inH₂O). The coarse-characterization results for Sensor 2-1 are shown in the graph in Fig. 4. The before-and-after fine-characterization results for the two.

LBA sensors are shown later in Figs. 11, 12. It is clear from the results in Fig. 4 that Sensor 2-1 has dramatically changed its calibration (output dropped by more than 50%), after 219 min, and has effectively completely failed by the end of the 20 hours of dust exposure. It is also clear (see Figs. 11, 12), that both LBA sensors' response curves are unchanged after 20 hours at 200 Pa.

The dramatic difference between Sensor 2-1 and the LBA sensors is not surprising, since the difference in flow impedance is a factor of at least 1000x, meaning over thousand times

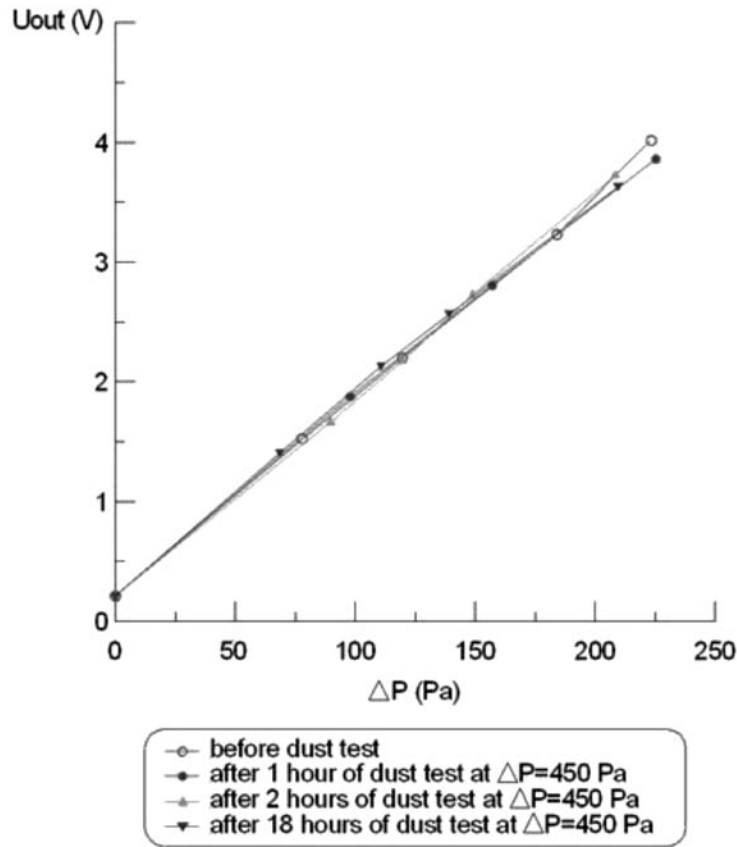


Fig. 7. Test #2 results for LBAS250UF6S (# 1) (horizontal orientation of the sensor)

more air volume went through Sensor 2-1, and also meaning that the flow velocity of dust-bearing air toward Sensor 2-1 was also >1000 times faster.

Note also that the few inches of transparent connection hoses to Sensor 2-1 had substantial visible dust residue within them, while far less dust residue was visible within the connection hoses to the LBA sensors.

Auxiliary Test #1a. As verification of this type of test, a separate 20-hour test was run on Sensor 2-3, along with another LBAS250UF6S sample, same type as the one used in Test#1.

The graphical results were very similar to those described above as shown in Figs. 4, 11. Sensor 2-3's output was drastically reduced after a few hours, and had dropped close to zero after 20 hours of dust exposure. Again, the LBA sample's output was effectively unchanged after the full 20 hours.

After this 20-hour test, the two samples were opened up (dissected) to find the failure

mechanism in Sensor 2-3. An abundance of agglomerated dust particles were found within the housing of Sensor 2-3, including a substantial quantity just inside the air inlet point. The tested LBA sensor housing was also opened up, and no dust was evident at the input port through which the air flowed before reaching the sensing element.

Test #2. In the second test, sensors LBAS250UF6S (# 1), and the same sensor LBAS050UF6S, Sensor 1-1 and Sensor 3-1 were connected in parallel to the dust chamber, in the first configuration shown in Fig. 2 (with the sensors arranged horizontally at the same level as the dust chamber). The test was run for 18 hours at a constant differential pressure $\Delta P = 450$ Pa (1.6 inH₂O). This applied pressure was close to the full-scale of Sensor 3-1, and above the full-scale of all of the other three sensors in the test, such that their output voltage was saturated during the test.

The coarse-characterization results are show

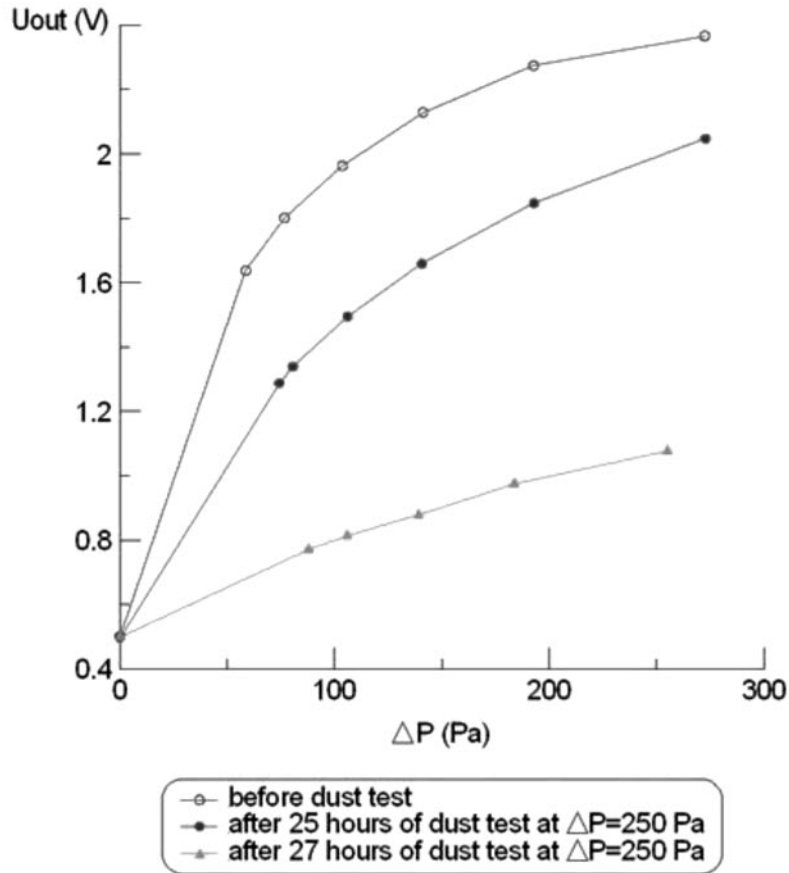


Fig. 8. Test #3 results for Sensor 2-2 (vertical orientation of the sensor)

in Figs. 5 to 7. The before-and-after fine characterization results for LBA samples are shown in Figs. 10 and 12. It is clear from the results in Fig. 5 that Sensor 1-1 has already significantly changed its calibration after 1 hour, and that its output has dropped by more than 50 % after 2 hours of exposure to dust-bearing air.

Note also that after 2 hours the zero-offset has also changed.

It is clear from the results in Fig. 6 that Sensor 3-1 has effectively completely failed between 2 hours and 18 hours of dust exposure.

Fig. 7 shows that the LBAS250UF6S (#1) sensor's coarse response curve is relatively unchanged after 1 hour, 2 hours, and 18 hours. Furthermore, the characterized before-and-after comparison in Fig. 10 confirms that indeed this sensor's response is unchanged after the full 18 hours of dust exposure.

Fig. 12 shows results for the LBAS050UF6S

sensor, which is the same sample that was used in the first comparison test described in TEST #1 earlier in this report. Again, the before-and-after measurements confirm that indeed this sensor's response is unchanged after the 18 hours plus previous 20 hours of dust exposure.

The dramatic difference between Sensors 1-1 and 3-1 and the LBA sensors is not surprising, since again the difference in flow impedance is two orders of magnitude or more. Again far more air volume went through Sensors 1-1 and 3-1, and again the flow velocity of dust-bearing air toward Sensors 1-1 and 3-1 was also many times faster.

Again, the few inches of transparent connection hoses to Sensors 1-1 and 3-1 had visible dust residue within them, while far less dust residue was visible within the connection hoses to the LBA sensors.

Test #3. In the third test, two LBA sensors

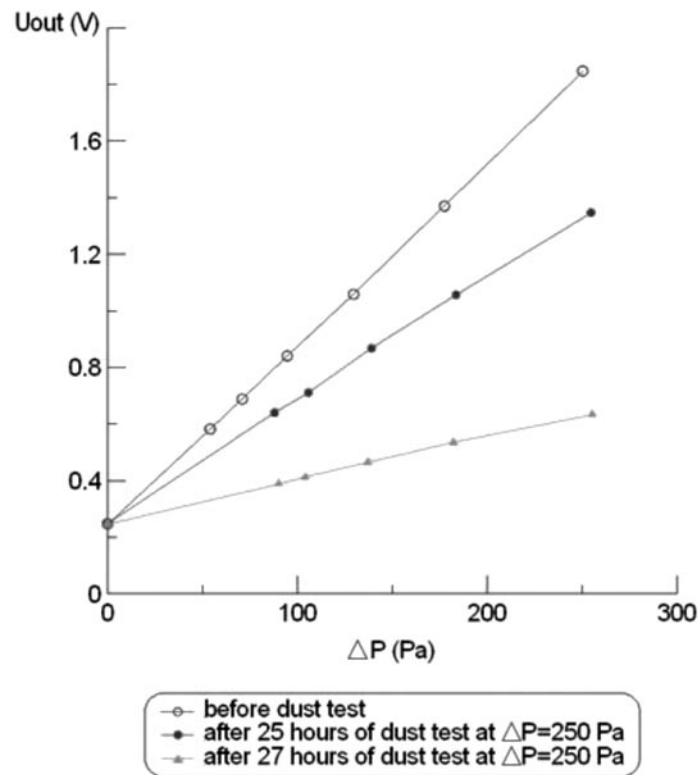


Fig. 9. Test #3 results for Sensor 3-2 (vertical orientation of the sensor)

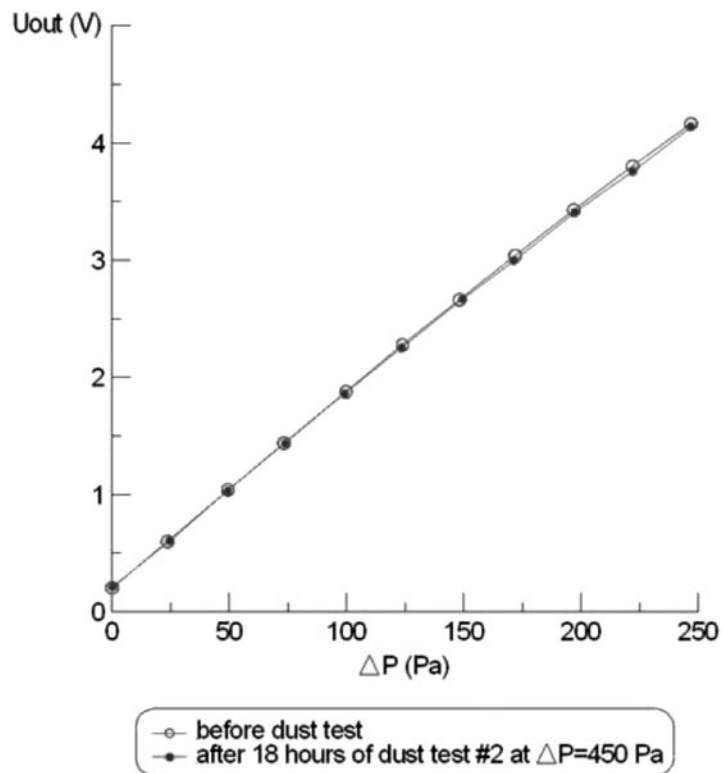


Fig. 10. Fine-characterization results for LBAS250UF6S (# 1)

already used in previous tests described above, sensor sample LBAS250UF6S (# 2), and sensor sample LBAS050UF6S, along with Sensor 2-2 and Sensor 3-2 were connected in parallel to the dust chamber, in the second configuration shown in Fig. 3 (with the sensors arranged vertically, above the dust chamber).

The test was run for 27 hours at a constant differential pressure $\Delta P=250$ Pa (1 inH₂O). This applied pressure was within the sensing range of Sensor 3-2, near the full-scale of LBAS250UF6S, and above the full-scale of the remaining two sensors in the test, such that their output voltage was saturated during the test.

The coarse-characterization results are shown in the graphs in Figs. 8 and 9. The before-and-after fine characterization results for LBA samples are shown in Figs. 11 and 12.

Note:

Both LBA sensors are the same sensor samples that were already exposed to many hours of dust-bearing air pressure in TEST #1 and TEST #2 above.

The results in Figs. 8 and 9 show that when the sensors are oriented vertically above the dust chamber, it takes much longer for the sensors under test to be affected. Sensor 2-2 and Sensor 3-2 have both significantly lost calibration after 25 hours, and have continued to lose calibration more severely after two more hours (total 27 hours of dust exposure for each sensor). This is not surprising, since the effect of gravity acts to delay and reduce the flow of dust particles upward toward the sensor inputs.

Fig. 11 shows that the LBAS250UF6S (#2) sensor's fine-characterized response curve is still unchanged after these additional 25 + 2 = 27 hours of dust exposure, beyond the original 20 hours of dust exposure from Test #1.

Fig. 12 shows that the LBAS050UF6S sensor may be finally beginning to change its calibration slightly (by a few per cent), after these additional 25 + 2 = 27 hours of dust exposure, beyond the original 20 + 18 = 38 hours of dust exposure from Test #1 and Test #2. It is not surprising that the

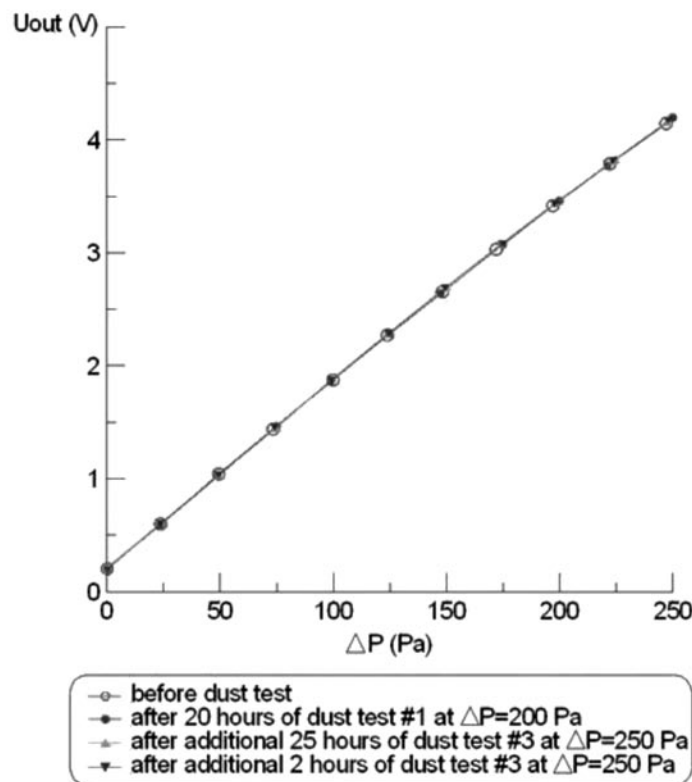


Fig. 11. Fine-characterization results for LBAS250UF6S (# 2)

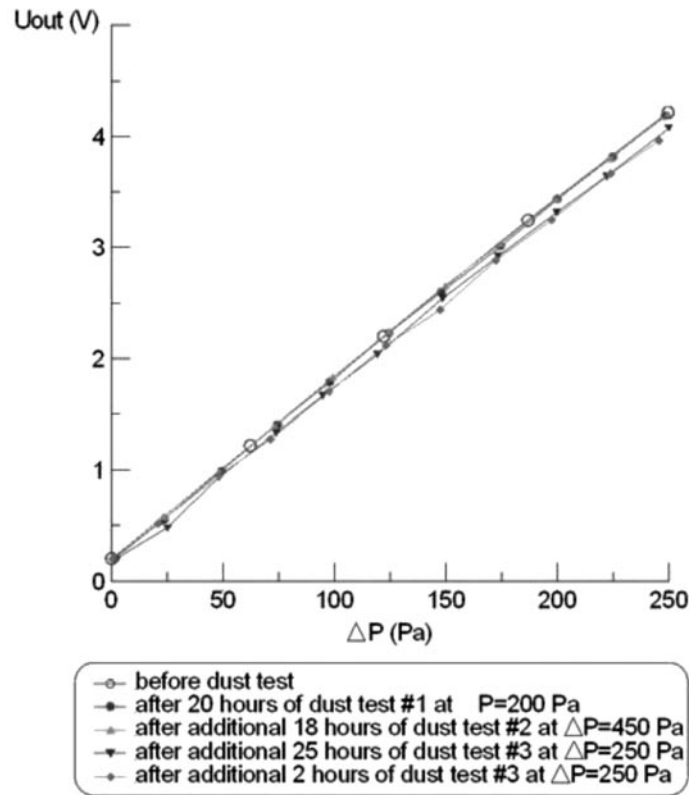


Fig. 12. Fine-characterization results for LBAS050UF6S

LBAS050UF6S sensor would begin to be affected before its neighbor LBAS250UF6S, because of its lower flow-impedance of ~ 30 kPa/(ml/s) vs. ~ 80 kPa/(ml/s).

Again, the dramatic difference between the Sensors 2-2 and 3-2, and LBA sensors is not surprising, since again the difference in flow impedance is two orders of magnitude or more. Again, far more air volume went through Sensors 2-2 and 3-2, and again the flow velocity of dust-bearing air toward Sensors 2-2 and 3-2 was also many times faster.

Again, the few inches of transparent connection hoses to Sensors 2-2 and 3-2, even when vertically oriented, had visible dust residue within them, while almost no dust residue was visible within the connection hoses to the LBA sensors. This is again consistent with the notion that the high flow-impedance of LBA sensors has limited the air-flow volume and velocity to such an extent that most of the dust has fallen out of suspension before reaching the LBA sensor.

Conclusions. For differential pressure (ΔP) sensors based on the thermal-anemometer sensing principle, involving small leakage through the sensor's airflow channel, the flow-impedance of that air-flow channel is an extremely important factor in determining the sensor's ease of use and immunity to dust-contamination.

With dust in the air flow, First Sensors LBA sensors having flow impedance >10 kPa/(ml/s) were compared directly with three other manufacturers' sensors using the same sensing principle, but having flow impedances of 15 Pa/(ml/s) to 300 Pa/(ml/s). In all cases the sensors having lower flow impedance lost calibration and/or failed completely after hours to tens of hours of normal operation. First Sensors LBA sensors did not show significant change of calibration.

The high flow impedance causes several effects:

- It reduces the volume of dust-bearing air which can approach the sensor's input;

- It reduces the velocity of air flow toward the sensor's input, allowing more dust to drop out of the flow before it reaches the sensor's input;

- It reduces the force on dust particles at the input of the sensor's flow channel.

When the air flow connection to the sensor is oriented vertically such that the flow of dust-bearing air must rise toward the sensor input, the effect of dust exposure is reduced.

Essentially, the less air-flow the sensor

requires through its body to make its measurement, the more ideal is the behavior of the sensor, and the better is the immunity to dust-bearing air. First Sensors LBA ΔP sensors provide very high flow impedance and therefore substantial advantages.

Potential users of thermal-anemometer-based ΔP sensors are invited to repeat the same or similar dust tests to verify suitability for use in the conditions of their own application(s).

THIEME, T. *Silicon Saxony e.V.*
01099, Dresden, Germany, Silicon Saxony e.V.
E-mail: info@silicon-saxony.de

ТИМЕ Торстен – директор по инновационным продуктам, «Кремниевая Саксония».
01099, Dresden, Germany, Silicon Saxony e.V.
E-mail: info@silicon-saxony.de